Proc. Natl. Acad. Sci. USA
Vol. 87, pp. 4093–4097, June 1990
Biochemistry

DNA binding properties of the purified Antennapedia homeodomain

(helix-turn-helix)

MARKUS AFFOLTER*, ANTHONY PERCIVAL-SMITH*, MARTIN MÜLLER*, WERNER LEUPIN†, AND WALTER J. GEHRING*

*Biozentrum, University of Basel, Klingelbergstrasse 70, CH-4056 Basel, Switzerland; and †Hoffmann–La Roche Cie. AG, CH-4002 Basel, Switzerland

Contributed by Walter J. Gehring, March 8, 1990

ABSTRACT **The *in vitro* DNA binding properties of a purified 68-amino acid Antennapedia homeodomain (Antp HD) peptide have been analyzed. Equilibrium and kinetic binding studies showed that stable DNA–protein complexes are formed with a K_d of 1.6×10^{-9} M and 1.8×10^{-10} M, respectively. Heterodimer analysis led to the conclusion that Antp HD interacts *in vitro* as a monomer with the DNA target sites used in our study. The results of methylation and ethylation interference studies indicated that the Antp HD closely approaches the target DNA primarily from one side in a region extending across three phosphate backbones. The DNA binding properties of the Antp HD and prokaryotic DNA binding domains that share a helix-turn-helix motif are compared.**

The homeobox is a 180-base-pair (bp) DNA segment first found in many developmental regulatory genes of *Drosophila* (1–3) and subsequently detected in other eukaryotes ranging from yeast to man (4, 5). It encodes a protein domain, the homeodomain (HD) present in many putative or well-characterized DNA regulatory proteins, the primary function of which seems to be site-specific recognition of DNA (5–9).

The three-dimensional structure of the Antennapedia homeodomain (Antp HD) has recently been determined by nuclear magnetic resonance spectroscopy in solution and shown to contain, at its C-terminal end, a structure virtually identical to the helix-turn-helix motif found in many prokaryotic repressors (10). However, the Antp HD differs from the prokaryotic repressors by having an additional fourth helix, which represents an extension of the helix-turn-helix motif. In the case of the bacterial gene regulatory proteins, x-ray crystallographic analysis of protein–DNA complexes (11–14) as well as functional studies using mutant protein and DNA target sites (15–17) revealed that amino acids within the second helical region of the helix-turn-helix generally contact groups exposed in the major groove of the target DNA. Therefore, this helix has been designated as recognition helix. The overall structural homology among helix-turn-helix motifs makes it possible in some cases to change the specificity of the protein–DNA interaction by altering the recognition helices (18).

Although the Antp HD does contain a helix-turn-helix motif, its structure shows important differences to the DNA binding domain of 434 (10, 11) or trp repressor (10, 19). Therefore, it was of interest to compare the DNA binding properties of the Antp HD with those of the prokaryotic helix-turn-helix DNA binding domains.

In this paper, we present a biochemical characterization of the DNA binding region of the Antp protein using purified Antp HD peptides. Our results suggest that the Antp HD and the prokaryotic repressor DNA binding domains interact with DNA in a substantially different manner.

The publication costs of this article were defrayed in part by page charge payment. This article must therefore be hereby marked "*advertisement*" in accordance with 18 U.S.C. §1734 solely to indicate this fact.

MATERIALS AND METHODS

Construction of Antp HD Expression Plasmids pAop2CS and pAop5. Construction of pAop2 is described in ref. 20. pAop2CS was generated by replacing the single cysteine codon in the Antp HD by a serine codon using site-directed mutagenesis. pAop5 was constructed by insertion of a 300-bp *Bal* I–*Bam*HI fragment of the Antp cDNA c909 (21) into the *Bam*HI site of pAR3040 (22). Expression of the cloned DNA fragment yields a protein of 117 amino acids of the following composition: 14 N-terminal amino acids derived from vector sequences, 102 amino acids derived from the Antp cDNA, as well as one additional vector-derived amino acid at the C terminus.

Expression and Purification of Peptides. All peptides were expressed in *Escherichia coli* BL21 (DE3) lysogen (22) and purified essentially as described (20). The 117-amino acid peptide used was purified from crude lysates by electrophoresis through a SDS/polyacrylamide gel (23). The protein concentration of the serine containing Antp HD was determined using an ε_{280} of 15,300 $cm^{-1} \cdot M^{-1}$.

Oligodeoxynucleotides. Purified single-stranded oligodeoxynucleotides were radioactively labeled with [α-^{32}P]dATP using Klenow polymerase (24).

The sequences of the filled-in, double-stranded oligodeoxynucleotides are (5′ → 3′):

BS1-26	ATGAAAGAAACACATTACGCTGCATG
BS2-26	AGCTGAGAAAAAGCCATTAGAGAAGC
BS2-18	GAGAAAAAGCCATTAGAG
BSX-18	ACAGGAGCAATTACAGCT
C-26	TCTTTTGTTTGGCCGGCAGCTACGAA
C-14	TGGCACCCTGACAA

The DNA concentration of oligodeoxynucleotides used in quantitative band shift assays was determined by direct absorption measurements at 260 nm. For interference studies, oligodeoxynucleotides BS1-26, BS2-26, and BSX-18 were subcloned in the *Sma* I site of the KS polylinker of Bluescript M13+ in both orientations, generating pBS1-26a, pBS1-26b, pBS2-26a, pBS2-26b, pBSX-18a, and pBSX-18b.

Mobility Shift Assays. Binding reactions were carried out in 20 μl of 20 mM Tris·HCl, pH 7.6/75 mM KCl/50 μg of bovine serum albumin per ml/1 mM dithiothreitol/10% glycerol and incubated at 20°C ± 1°C (unless stated otherwise). The samples were run at room temperature on native, 15% polyacrylamide gels (20). For saturation experiments, gel slices corresponding to free and bound DNA were cut out, incubated 10 hr at 55°C in 1 ml of Protosol, and then quantified by liquid scintillation spectroscopy. The binding reaction for the interference studies using subcloned oligodeoxynucleotides contained 1 ng of Bluescript DNA per μl as competitor.

Interference Studies. *Hin*dIII–*Xba* I DNA fragments 3′ end-labeled at the *Hin*dIII site were isolated from pBS1-26a,

Abbreviation: Antp HD, Antennapedia homeodomain.

pBS1-26b, pBS2-26a, pBS2-26b, pBSX-18a, and pBSX-18b, treated with ethyl nitrosourea, and subsequently cleaved at modified phosphates as described (25). Dimethyl sulfate treatment and subsequent cleavage with 0.1 M NaOH were done as published (26).

RESULTS

Determination of the Equilibrium Binding Constant. With oligodeoxynucleotides derived from binding sites identified ≈2 kilobases (kb) upstream of the *Drosophila* engrailed gene promoter and a mobility shift assay, we detected specific and stable Antp HD–DNA complexes with a 68-amino acid Antp HD peptide (20). To avoid the formation of disulfide bridges leading to "artificial" dimerization (20), the single cysteine of the Antp HD present in the turn of the helix-turn-helix motif was replaced by a serine. All of the properties of the binding reaction presented here are unchanged by this mutation. We designate the peptide encoded by the T7-inducible transcript of pAop2CS as "Antp HD."

The equilibrium dissociation constant (K_d) was determined from Antp HD saturation experiments (Fig. 1*a*) using the oligodeoxynucleotide BS2-18 (see *Materials and Methods*) as the ligand. The K_d was 1.6×10^{-9} M at 20°C. Conversely, by varying the concentration of Antp HD with a fixed, limiting amount of BS2 (see Fig. 3; see also legend), the K_d was estimated to be in the order of $1–2 \times 10^{-9}$ M, which agrees closely with the saturation experiment. [Note that this K_d is about 10-fold lower than previously reported (20); this is due to an overestimation of the protein concentration with the Bio-Rad assay and to the different incubation temperature.] The total concentration of bound Antp HD was 11 nM ± 0.8 nM (see Fig. 1 legend). This is about equal to the input concentration of 10 nM, indicating that essentially all of the Antp HD molecules in the peptide preparation are active and bind DNA. Since the amount of bound BS2-18 was used to calculate $[HD]_o$ (see Fig. 1 legend), the close agreement between input concentration and bound concentration suggests that the complex is composed of equal molar amounts of each component.

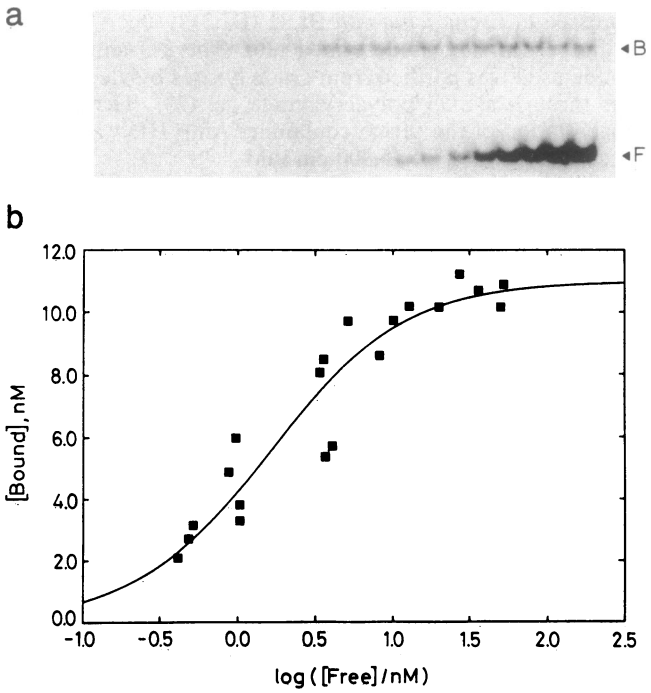

FIG. 1. Saturation experiments. Antp HD at a fixed concentration of 10 nM was incubated for 4 hr in binding buffer containing increasing concentrations of labeled BS2-18. Bound (B) and free (F) DNAs were visualized by autoradiography (*a*). Data obtained from the titration in *a* are plotted in *b*. The following equilibrium equation was fitted to the data by nonlinear least-squares in order to calculate $[HD]_o$ and K_a:

$$[\text{HD-DNA}] = \frac{[HD]_o \cdot K_a([DNA]_o - [\text{HD-DNA}])}{1 + K_a([DNA]_o - [\text{HD-DNA}])}.$$

$[HD]_o$ and $[DNA]_o$ are the total concentrations of Antp HD and BS2-18, respectively, and [HD-DNA] is the concentration of the complex between the two. K_a is the association constant. The errors of the K_a and the $[HD]_o$ were determined by the linear approximation. The values obtained were $K_a = (0.63 \pm 0.19) \times 10^9\ M^{-1}$ and $[HD]_o = (11 \pm 0.8) \times 10^{-9}$ M.

Kinetic Studies of the Interaction Between Antp HD and DNA. The stability of the Antp HD–DNA complex was measured in competition experiments (Fig. 2*a*; see legend for description of the experiment). Analysis of the data shown in Fig. 2*a* yielded a dissociation rate constant (k_d) of $(1.3 \pm 0.09) \times 10^{-4}\ sec^{-1}$ and a half-life for the complex of 89 min. The association rate constant (k_a) was also measured in a combined binding/competition assay (see Fig. 2 legend), and a best fit for the time-dependent association observed (Fig. 2*b*) was $(7.4 \pm 0.8) \times 10^5\ M^{-1} \cdot sec^{-1}$. The competition experiment shown in Fig. 2*c* demonstrates that the 200-fold excess of unlabeled BS2-18 added to both sets of kinetic experiments was sufficiently high to competitively inhibit the labeled BS2-18 in the binding reaction.

The K_d for a bimolecular reaction is equal to k_d/k_a. Using the data obtained from the kinetic experiments, we calculated the K_d to be 1.8×10^{-10} M. This is almost 9 times lower than the value of 1.6×10^{-9} M obtained by protein or DNA titration experiments. We do not know the reason for this discrepancy. However, since all of the kinetic assays were performed in the presence of high amounts of unlabeled competitor DNA, the binding parameters might have slightly changed.

Specific Versus Nonspecific DNA Binding. To estimate the affinity of the Antp HD for nonspecific DNA, we had previously synthesized a 26-bp oligodeoxynucleotide, C-26 (20). To estimate the apparent K_d of the Antp HD interaction with nonspecific sequences, a mixture of limiting amounts of specific and nonspecific oligodeoxynucleotides was incubated with increasing amounts of Antp HD (Fig. 3). Consistent with the results obtained in the saturation experiment, the K_d for BS2-18 was $1–2 \times 10^{-9}$ M. Much higher protein concentrations were required to bind half of C-26 ($0.6–1.0 \times 10^{-7}$ M). The K_d of a shorter nonspecific DNA fragment, namely C-14, was even somewhat higher ($2–4 \times 10^{-7}$ M).

Stoichiometry of the Antp HD–DNA Complexes. On the basis of ultracentrifugation studies, we previously concluded that the purified 68-amino acid Antp HD peptide existed as a monomer in solution (20). Using ultracentrifugation analysis, a longer, 117-amino acid Antp HD-containing peptide (see *Materials and Methods*) was also shown to exist as a monomer in solution under reducing conditions (measured by A. Lustig, personal communication). This 117-amino acid peptide forms a specific complex with BS2-26 (Fig. 4, lane 2). This complex migrates more slowly than the complex of BS2-26 with the 68-amino acid Antp HD (Fig. 4, compare lanes 2 and 9). The properties of the two peptides behaving as monomers in solution and of the DNA–protein complex exhibiting different mobility in a gel retardation analysis allowed us to assay the stoichiometry of the complex by looking for heterodimer formation. In this analysis an increasing amount of the 68-amino acid Antp HD was added to a constant amount of 117-amino acid Antp HD in the binding reaction. If more than one protein would interact with BS2, formation of complexes that migrate to an intermediate position between the 68-amino acid and the 117-amino acid complexes would be expected; since no such complexes were detected (Fig. 4) and since the proteins exist as monomers in

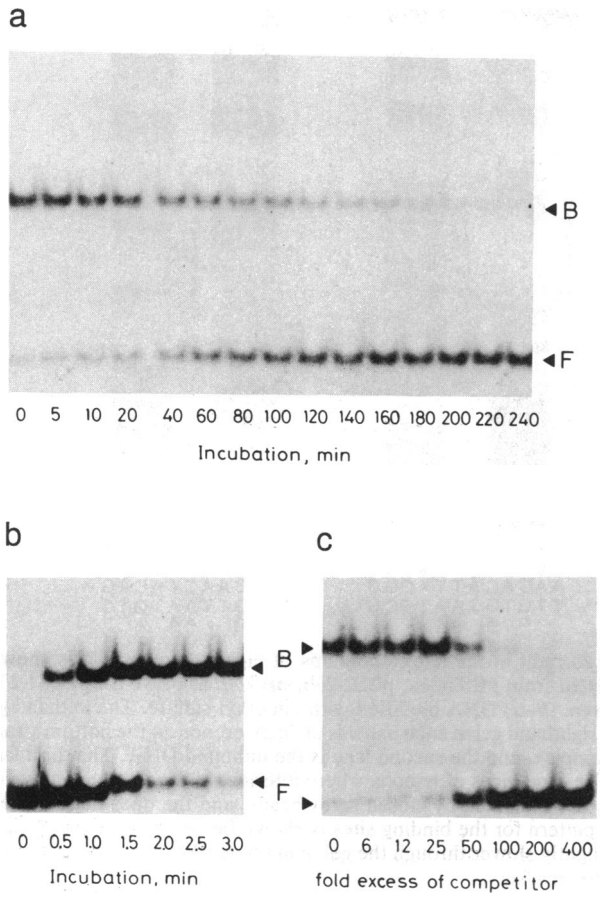

FIG. 2. Kinetic studies on Antp HD–DNA interaction. (*a*) Measurement of the dissociation kinetics. Antp HD and labeled BS2-18 were incubated at 20°C for 4 hr at final concentrations of 2×10^{-8} and 2×10^{-9} M, respectively. A 200-fold excess of unlabeled BS2-18 (over labeled BS2-18) was then added and incubation proceeded for the indicated time period. Bound (B) and free (F) DNAs were quantified by densitometry. k_d was calculated with the following equation: $-k_d t = \ln[\text{HD-DNA}]/[\text{HD-DNA}]_o$ (27), where $[\text{HD-DNA}]_o$ represents the amount of the complex present immediately after adding of unlabeled BS2-18. The value determined using linear least-squares analysis was $(1.3 \pm 0.09) \times 10^{-4}$ sec^{-1}, which represents a half-life of the complex of 89 min. (*b*) Measurements of the association kinetics. Antp HD and labeled BS2-18 were mixed at time 0 at final concentrations of 2×10^{-8} M and 2×10^{-9} M, respectively. After a short incubation at 20°C, the association reaction of HD and labeled DNA was stopped by the addition of a 200-fold excess of unlabeled BS2-18. Free (F) and bound (B) DNAs were quantified by densitometry and the k_a was calculated with the following equation:

$$k_a t = \frac{1}{[\text{HD}]_o - [\text{DNA}]_o} \ln \frac{[\text{DNA}]_o([\text{HD}]_o - [\text{HD-DNA}])}{[\text{HD}]_o([\text{DNA}]_o - [\text{HD-DNA}])}.$$

The best fit obtained for the k_a was $(7.4 \pm 0.8) \times 10^5$ M^{-1}·sec^{-1}. (*c*) Competition experiment. Antp HD and labeled BS2-18 were incubated at final concentrations of 2×10^{-8} M and 2×10^{-9} M, respectively, in the presence of increasing concentrations of unlabeled BS2-18. The 6-fold excess of BS2-18 corresponds to 1.2×10^{-8} M. The samples were incubated for 2 hr at 20°C.

solution, we conclude that one HD-containing protein interacts with one oligodeoxynucleotide, consistent with the saturation analysis.

Ethylation and Methylation Interference Studies. To characterize the interaction of Antp HD with its target DNA, ethylation and methylation interference studies were performed. In the ethylation interference experiment, two 67-bp DNA fragments, each containing the BS2 binding site in a different orientation, were 3′ end-labeled and modified with

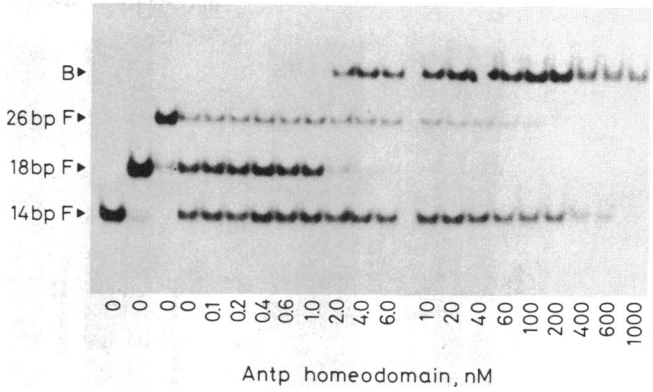

FIG. 3. Specificity of binding. Mixtures of three labeled oligodeoxynucleotides, C-26 (26 bp), BS2-18 (18 bp), and C-14 (14 bp), each present at a final concentration of 2×10^{-10} M, were incubated with increasing concentrations of Antp HD for 4 hr at 20°C. The first three lanes serve as size markers. B, bound; F, free.

ethyl nitrosourea. The ethylated DNA was incubated with Antp HD, and the Antp HD–DNA complex was separated from the unbound DNA by gel retardation. The bound DNA and unbound DNA were isolated and cleaved specifically at the modified phosphates.

The ethylations that inhibit Antp HD from binding were visualized on the sequencing gel as a loss of a band in the bound lane relative to the unbound lane (Fig. 5*a*). Phosphate triester formation with ethyl nitrosourea adds an ethyl group and removes a negative charge. Hence, an inhibition of Antp HD binding can be due to either a steric interference or a loss of an electrostatic interaction between the Antp HD and a charged phosphate. On the top strand of BS2, ethylation at 6 positions inhibits Antp HD binding. Five of the 6 positions are clustered together, with the sixth position being 5 positions 3′ to this cluster. On the bottom strand of BS2, ethylation of 5 adjacent positions inhibits binding. Of the total of 11 positions that inhibit binding, 7 abolish binding and 4 diminish binding. The positions that interfere with binding when mapped on a projection diagram of idealized B-DNA indicate that the Antp HD interacts primarily with one face of B-DNA and across three sugar-phosphate backbones (Fig. 6).

The methylation interference experiments were performed in a similar manner as the ethylation interference experiments, except that the DNA was modified with dimethyl sulfate. Since dimethyl sulfate only methylates the N-3 of adenine and the N-7 of guanine of double-stranded DNA,

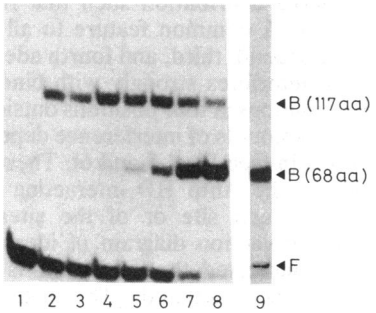

FIG. 4. Heterodimer analysis. Constant amounts of an Antp HD peptide of 117 amino acids (lanes 2–8) were incubated with increasing amounts of the 68-amino acid Antp HD peptide (lanes 3–8). After a 15-min incubation period on ice, labeled BS2-26 was added and incubation was continued for 2 hr. No protein was added to the sample run in lane 1; only Antp HD was added to the sample run in lane 9. The complexes formed with the extended Antp HD [B (117 amino acids)] and the shorter Antp HD [B (68 amino acids)] are indicated. B, bound; F, free.

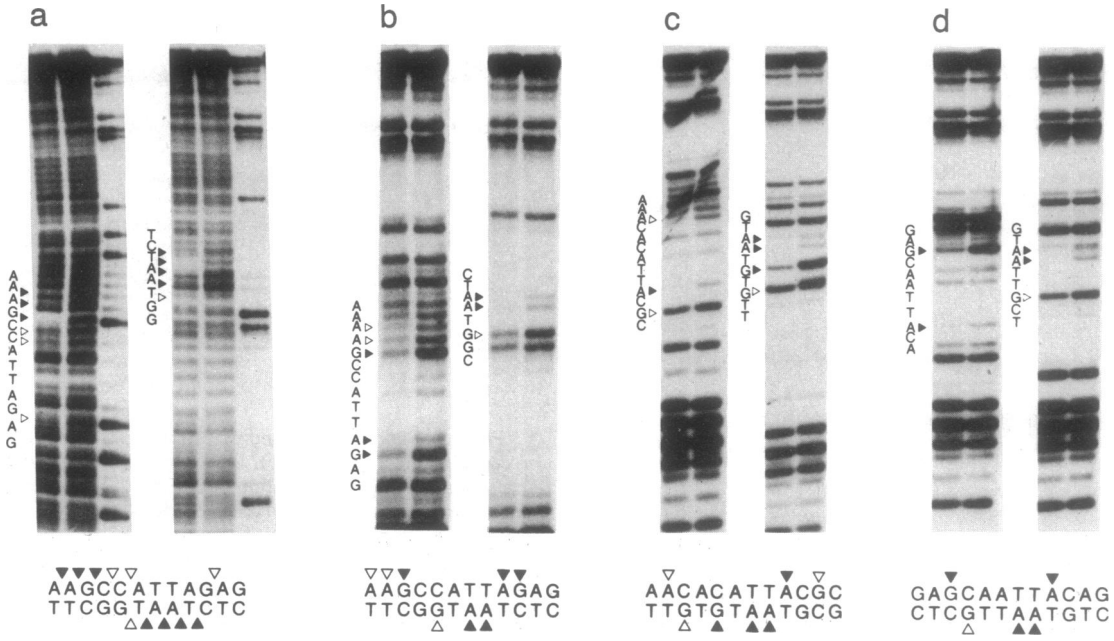

FIG. 5. Ethylation and methylation interference experiments. From left to right in the autoradiograms of eight sequencing gels shown, *Hin*dIII–*Xba* I DNA fragments (3′ end-labeled at the *Hin*dIII site) were isolated from pBS2-26a, pBS2-26b, pBS2-26a, pBS2-26b, pBS1-26a, pBS1-26b, pBSX-18a, and pBSX-18b. (*a*) DNA modified with ethyl nitrosourea. (*b–d*) DNA modified with dimethyl sulfate. The lefthand gel in each panel is an interference experiment on the top strand of DNA, and the righthand gel in each panel is an interference on the bottom strand of the DNA. The first lane of each gel is the DNA isolated from the bound complex, and the second lane is the unbound DNA. The third lane in the gels shown in *a* is the marker lane of dimethyl sulfate-treated DNA. The sequences of regions where interferences occur are shown on the left of each gel. The modified phosphates or bases that interfere strongly are indicated by closed arrowheads, and the ones that interfere weakly are indicated by open arrowheads. The summary of the interference pattern for the binding sites is shown below the autoradiograms. In the ethylation interference experiments the modified phosphate migrates slightly slower through the gel than the marker, but a side reaction product of ethyl nitrosourea, particularly strong at adenines, migrates with the marker.

only few areas of the surface of a binding site can be assayed for methylation interference. To increase the surface area of DNA assayed, we performed methylation interference studies on three Antp HD binding sites: BS1 and BS2, from the engrailed promoter (20), and BSX from the ftz enhancer (28). These sites differ in sequence at many positions around the sequence 5′-ATTA-3′ found in all three sites. The sequencing gels of the methylation interference experiments with BS2, BS1, and BSX are shown in Fig. 5 *b*, *c*, and *d*, respectively. Interpretation of the methylation interference pattern is more difficult than interpretation of the ethylation interference pattern. The alkylation, apart from adding a methyl group, adds a positive charge and changes the resonance state of the adenine and guanine ring (29). Hence, interference of Antp HD binding can be due to a steric exclusion of binding or a change in the charge distribution such that the Antp HD cannot recognize it. A common feature to all sites is that methylation at the second, third, and fourth adenosine of the 5′-ATTA-3′ motif interferes strongly with binding (Fig. 5). Conversely, methylations at four positions outside the ATTA motif gave varying amounts of interference depending on the site that position is in (see Figs. 5 and 6). These differences may be a result of the Antp HD interacting in a slightly different way with each site or of the sites varying in structure. On the projection diagram of idealized B-DNA (Fig. 6), we have indicated the methylations that do not interfere along with the ones that do. The projection diagram shows that methylation of groups in two minor grooves and the adjacent two major grooves interfere with binding. Also, these interferences are clustered around the phosphates that interfere with binding when ethylated.

DISCUSSION

By using a mobility shift assay with purified Antp HD peptide and DNA segments we have shown that the *E. coli*-expressed Antp HD binds *in vitro* as a monomer with a relatively high affinity ($K_d \leq 1.6 \times 10^{-9}$ M) to the site it recognizes specifically. Several independent assays provide evidence that the complex is of monomeric composition. The heterodimer analysis with HD-containing peptides that behave as monomers in solution (as determined by ultracentrifugation studies) fails to give rise to heterodimeric complexes (Fig. 4). Antp HD saturation experiments (Fig. 1) as well as the lack of symmetry of chemically modified functional groups on the DNA molecule that interfere with binding (Figs. 5 and 6) also support the conclusion that a single Antp HD molecule interacts with the binding site used in this study.

More detailed information on Antp HD interactions with DNA was obtained in interference studies. Ethylation interference experiments revealed that 11 phosphate groups interfere with binding when ethylated (Figs. 5 and 6). These phosphates are displayed predominantly on one side of an idealized B-DNA molecule and indicate that Antp HD closely approaches DNA in a region extending across three phosphate backbones. In hydroxyl radical protection experiments, the yeast HD-containing Mat α2 protein also protected three adjacent phosphate sugar backbones of its binding site from cleavage (30). Our methylation interference studies with three Antp HD binding sites show that the positions that interfere with binding extend over 10 bp of DNA and are clustered around the phosphates that interfere when ethylated. Absence of interference in flanking sequences confirms the specificity of Antp HD binding.

There is a considerable difference in the affinity of Antp HD for its site and in the stability of the resulting complex (this study), with the affinity of several prokaryotic helix-turn-helix DNA binding domains for their monomer (half-operator) binding sites and the stability of the resulting complexes (31–34). In general, dissociation constants for half-operator interactions have been estimated to be in the

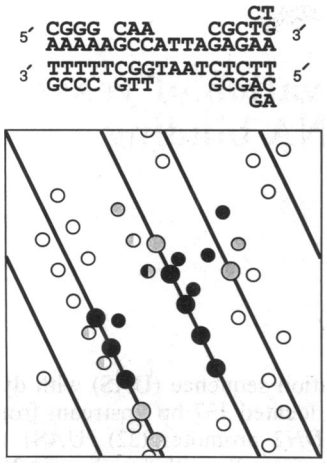

FIG. 6. Projection diagram summary of the ethylation and methylation interference data. The diagram represents the projection of chemical groups of DNA on to a cylindrical surface, which is then cut along its *z* axis and folded out. The sequence at the top is that of BS2 with the different bases present in BS1 and BSX above and below it. The shared 5′-ATTA-3′ motif was used to align the three sites relative to one another. The ethylation interferences of BS2-26 are indicated as the larger shaded circles along the sugar phosphate backbone (the diagonal lines). The positions of the N-3 of the adenines and of the N-7 of the guanines that were assayed for methylation interference are indicated in the minor and major groove, respectively, by the smaller circles. Positions that did not interfere in the methylation studies are not filled in. Phosphates that did not interfere when ethylated are not shown. Weak interferences are indicated by stippled circles, and strong interferences are indicated by solid circles. Interferences that behave differently depending on the binding site the group is in are indicated as half-filled circles.

order of 10^{-5} to 10^{-6} M and the half-lives of those complexes have been estimated to be equal to or less than seconds. With purified 434 and P22 repressor DNA binding domains and the corresponding radioactively labeled half-operator target sites, we only detected trace amounts of complexes formed at protein concentrations $\geq 10^{-5}$ M, demonstrating that our conditions do not artifically stabilize protein–DNA complexes (M.A., G. Otting, D. Neri, and K. Wüthrich, unpublished results). Kinetic studies of the Antp HD binding reaction suggest that the dramatic difference in the affinities of Antp HD and prokaryotic DNA binding domains is due to the low dissociation rate of the Antp HD–DNA complex. Antp HD also has a relatively high affinity for nonspecific DNA ($K_d \approx 10^{-6}$–10^{-7} M, Fig. 3), suggesting that nonspecific interactions with DNA might promote the high stability of the complex. A structural feature unique to the Antp HD is helix 4 that "elongates" the third, putative recognition helix by an additional 7 amino acids (10). This region, which is part of the most conserved region of the homeodomain and contains 4 or 5 lysines or arginines (4, 5), has been shown to be absolutely required for stable complex formation (A.P.-S. and W.J.G., unpublished). It is possible that helix 4 is an important structural feature partly responsible for the formation of the extremely stable complexes that Antp HD forms with its target.

The binding studies presented here argue that the Antp HD and prokaryotic repressor DNA binding domains interact with DNA in a substantially different manner. To what extent this difference will relate to differences observed at the structural level of the Antp HD–DNA complex remains to be seen. It is interesting to note, however, that it has already been suggested that the putative recognition helix of homeodomain proteins is oriented differently in the major groove than the recognition helix of bacteriophage repressor proteins (35, 36), because of the importance of position 9 of the third helix in determining DNA binding specificity.

We are indebted to Ariel Lustig for carrying out the ultracentrifugation analysis. We are most grateful to Charles Robert for analysis of binding data and for invaluable discussions. M.A. thanks Henry Krause for communication of unpublished results on the presence of HD binding sites. Special thanks go to Erika Wenger-Marquardt for typing the text and to Liselotte Müller and Margrit Jaeggi for graphic art work. A.P.-S. is a Medical Research Council (Canada) fellow. This work was supported by the Kantons Basel and the Swiss National Science Foundation.

1. McGinnis, W., Levine, M. S., Hafen, E., Kuroiwa, A. & Gehring, W. J. (1984) *Nature (London)* **308,** 428–433.
2. McGinnis, W., Garber, R. L., Wirz, J., Kuroiwa, A. & Gehring, W. J. (1984) *Cell* **38,** 403–409.
3. Scott, M. P. & Weiner, A. J. (1984) *Proc. Natl. Acad. Sci. USA* **81,** 4115–4119.
4. Gehring, W. J. (1987) in *Molecular Approaches to Developmental Biology*, eds. Firtel, R. & Davidson, E. (Liss, New York), pp. 115–129.
5. Scott, M. P., Tamkun, J. W. & Hartzell, G. W. (1989) *Biochim. Biophys. Acta* **989,** 25–48.
6. Levine, M. & Hoey, T. (1988) *Cell* **55,** 537–540.
7. Struhl, K. (1989) *Trends Biochem. Sci.* **14,** 137–140.
8. Wright, C. V. E., Cho, K. W. Y., Oliver, G. & De Robertis, E. M. (1989) *Trends Biochem. Sci.* **14,** 52–56.
9. Schaffner, W. (1989) *Trends Genet.* **5,** 37–39.
10. Qian, Y. Q., Billeter, M., Otting, G., Müller, M., Gehring, W. J. & Wüthrich, K. (1989) *Cell* **59,** 573–580.
11. Aggarwal, A. K., Rodgers, D. W., Drottar, M., Ptashne, M. & Harrison, S. C. (1988) *Science* **242,** 899–907.
12. Jordan, S. R. & Pabo, C. O. (1988) *Science* **242,** 893–899.
13. Wolberger, C., Dong, Y., Ptashne, M. & Harrison, S. C. (1988) *Nature (London)* **335,** 789–795.
14. Otwinowski, Z., Schevitz, R. W., Zhang, R.-G., Lawson, C. L., Joachimiak, A., Marmorstein, R. Q., Luisi, B. F. & Sigler, P. B. (1988) *Nature (London)* **335,** 321–329.
15. Pabo, C. O. & Sauer, R. T. (1984) *Annu. Rev. Biochem.* **53,** 293–321.
16. Schleif, R. (1988) *Science* **241,** 1182–1187.
17. Brennan, R. G. & Matthews, B. W. (1989) *J. Biol. Chem.* **264,** 1903–1906.
18. Wharton, R. P. & Ptashne, M. (1985) *Nature (London)* **316,** 601–605.
19. Lawson, C. L., Zhang, R. G., Schevitz, R. W., Otwinowski, Z., Joachimiak, A. & Sigler, P. B. (1988) *Proteins* **3,** 18–31.
20. Müller, M., Affolter, M., Leupin, W., Otting, G., Wüthrich, K. & Gehring, W. J. (1988) *EMBO J.* **7,** 4299–4304.
21. Schneuwly, S., Kuroiwa, A., Baumgartner, P. & Gehring, W. J. (1986) *EMBO J.* **5,** 733–739.
22. Studier, F. W. & Moffatt, B. A. (1986) *J. Mol. Biol.* **189,** 113–130.
23. Hager, D. A. & Burgess, R. R. (1980) *Anal. Biochem.* **109,** 76–86.
24. Maniatis, T., Fritsch, E. F. & Sambrook, J. (1982) *Molecular Cloning: A Laboratory Manual* (Cold Spring Harbor Lab, Cold Spring Harbor, NY).
25. Siebenlist, U. & Gilbert, W. (1980) *Proc. Natl. Acad. Sci. USA* **77,** 122–126.
26. Maxam, A. M. & Gilbert, W. (1977) *Proc. Natl. Acad. Sci. USA* **74,** 560–564.
27. Kim, J. G., Takeda, Y., Matthews, B. W. & Anderson, W. F. (1987) *J. Mol. Biol.* **196,** 149–158.
28. Pick, L., Schier, A., Affolter, M., Glenewinkel, T. & Gehring, W. J. (1990) *Genes Dev.*, in press.
29. Lawley, P. D. & Brookes, P. (1963) *Biochem. J.* **89,** 127–128.
30. Sauer, R. T., Smith, D. L. & Johnson, A. D. (1988) *Genes Dev.* **2,** 807–816.
31. Ogata, R. T. & Gilbert, W. (1978) *Proc. Natl. Acad. Sci. USA* **75,** 5851–5854.
32. Fried, M. & Crothers, D. M. (1981) *Nucleic Acids Res.* **9,** 6505–6525.
33. Pabo, C. O. & Lewis, M. (1982) *Nature (London)* **298,** 443–447.
34. Hollis, M., Valenzuela, D., Pioli, D., Wharton, R. & Ptashne, M. (1988) *Proc. Natl. Acad. Sci. USA* **85,** 5834–5838.
35. Hanes, S. D. & Brent, R. (1989) *Cell* **57,** 1275–1283.
36. Treisman, J., Gönczy, P., Vashishtha, M., Harris, E. & Desplan, C. (1989) *Cell* **59,** 553–562.